10 years of X-ray variabiliy in the Chandra Deep Field South

M. Paolillo (Univ.Federico II of Naples), I. Papadakis (Univ. of Crete), N.Brandt (PSU), V.Allevato (Univ.Federico II of Naples, MPE), A.Comastri (INAF-OABo), R. Giacconi (JHU), E. Schrier (JHU-AURA) and the CDFS team

The long observing campaign of the *Chandra Deep Field South* allows to study AGN variability up to z~5 over a 10 year baseline. We find that variability is an ubiquitous property of AGNs which is detectable whenever sufficient statistic is available. We use Monte-Carlo simulations to account for biases introduced by the discontinous sampling and the low-count regime. The variability properties of our population are similar to what is expected based on nearby AGNs, due to the physics of the accretion process. Only for a handful of sources we observe spectral changes consistent with variations in the obscuring column dęnşity. However we show that simple models based on dependence of the PSD on BH mass and accretion rate still fail to account for the observed luminosity and redshift trends.

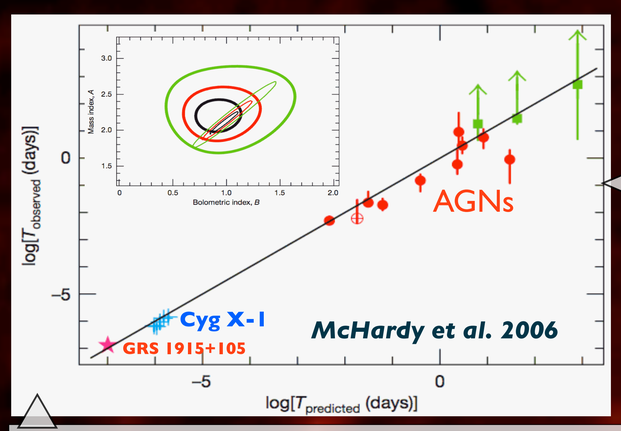

Fig.1: Predicted break timescales compared to the observed ones. $T_{predicted}$ is derived from the the best fit (see inset) relationship to the combined sample of AGN and GBHs: log T_B = 2.1 log M_{BH} - 0.98 log L_{bol} - 2.32.

Introduction

Our current understanding of the temporal properties of Active Galactic Nuclei are mainly based on a small sample of bright and nearby sources for which long monitoring campaigns have been possible. Recent work on nearby AGNs has shown that X-ray variability presents a characteristic timescale in the form of a break in the Power Density Spectrum, strengthening the link between galactic BH and SMBH (Markowitz et al. 2003; also see Uttley et al. 2002; Mc Hardy et al. 2004). While the origin of such feature is still unclear, it has been suggested (**Fig.1**, McHardy et al.2006) that it correlate with BH mass and accretion rate, possibly following the relation:

$$t_{Break} \propto (M_{BH})^A / (L_{bol})^B$$

The extension of these results to distant AGNs is difficult due to the sparse sampling and the low statistics which do not allow to derive high quality PDS.

CDFS X-ray Data and Lightcurve extraction

The Chandra Deep Field South (CDFS) dataset is described in Luo et al. (2008) and Xue et al. (2011). It consists of 54 observations collected by Chandra between 1999 and 2010, adding up to a total exposure time of 3.8 Ms; the individual observations have durations ranging from ~10 ks up to 141 ks. The data were reduced following Tozzi et al. (2006), to create event list and exposure maps in the 0.5-8, 0.5-2 and 2-8 keV bands. We extract lightcurves as done in Paolillo et al. (2004) for the 1 Ms dataset. We start from the main source catalog of Xue et al. (2011), consisting in 740 X-ray sources. For each source we measured counts within a circular aperture with variable radius R_S depending on the distance from the average aimpoint: R_S = 2.4×FWHM arcsec, where FWHM=$\sum_{i=0,2}$ $a_i\theta_i$ with a={0.678,−0.0405,0.0535}. The local background for each source was measured in a nearby circular annulus. We binned the data into individual observations: this allows to derive lightcurves with 54 points over a 10 years interval. In total 673 (91%) of our sources have lightcurves with at least 25 bins and 564 (76%) are sampled by all 54 observations. The lightcurves were extracted both in the full 0.5-8 keV band, as well as in the 0.5-2 and 2-8 keV bands in order to study the spectral variability of our sources; we further extracted lightcurves in the 2-8 keV rest-frame band for sources with available redshift 2. An example of the CDFS lightcurves is shown in **Fig.2**.

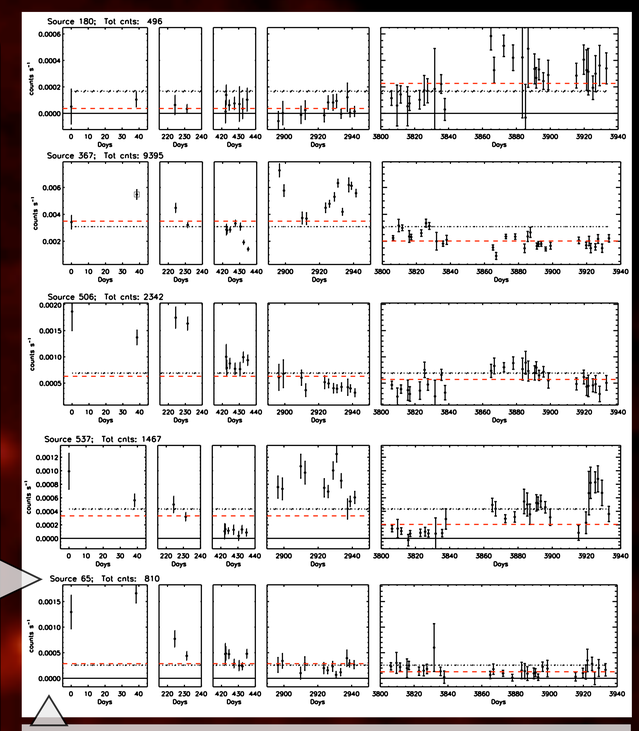

Fig.2: Example of CDFS lightcurves in the 0.5-8 keV band, for sources of different flux and temporal behavior. The average count rate and error are marked by a continuous line and hatched region respectively. Faint AGN detection does depend on variability: some are undetected within observing campaigns of just a few days!

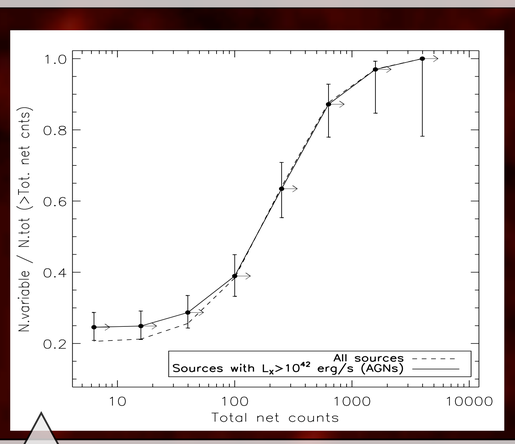

Fig.3: Cumulative fraction of variable sources in the CDFS, as a function of the net source counts. The number of variable sources increases at higher counts (i.e. S/N) .Errorbars represent the 95% binomial uncertainty.

Variability behavior and timescales

Comparing with simulations of constant sources, we find that 140 out of 740 (19%) sources are variable with Prob>95% . This fraction however is both affected by the low statistic of the majority of the sources (70 median counts), and the contamination by normal galaxies with L_X<10^{42} erg s^{-1}. In Figure 3 we plot the cumulative fraction of variable sources, showing that at high count levels all sources are found to vary. The plot confirms the trend observed by Paolillo et al. (2004) in the 1 Ms dataset, and Young et al. (2011) in the 4 Ms data with lower time resolution, that variability is more easily detected in higher S/N sources and supports the view that all AGNs are intrinsically variable on a broad range of timescales.

The red-noise nature of CDFS AGNs is reflected in **Fig.4**. The likelihood of detecting variability on a specific timescale increases toward longer timescales in the source rest-frame. In addition the vast majority (~ 75%) of AGNs display significant variability on short timescales (<1 day), with the totality of the population variable on timescales <3 days, thus indicating that part of the emission is produced in regions consistent with the size of the inner accretion disk and the broad-line region. The redshift distribution of variable and non-variable sources is shown in **Fig.5**.

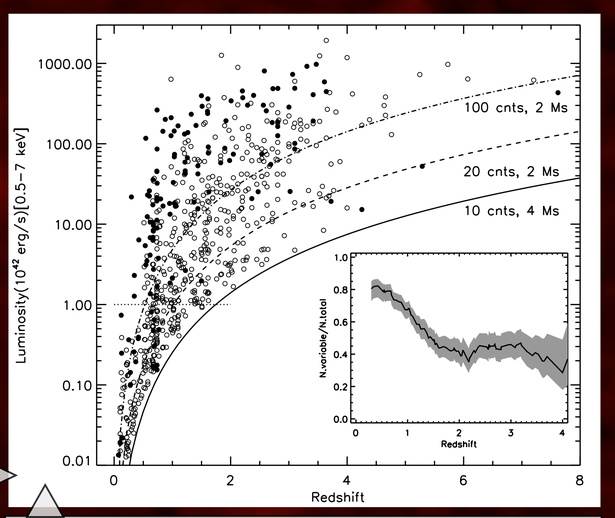

Fig.5: X-ray luminosity vs redshift. Solid dots mark variable sources. The curves highlight three limits characterizing the survey, (solid: at the aimpoint, dashed: the average across the FOV, dot-dashed: the average limit for variability detection). The horizontal dotted line marks the L_X = 10^{42} erg s^{-1} limit used to discriminate AGNs from galaxies.

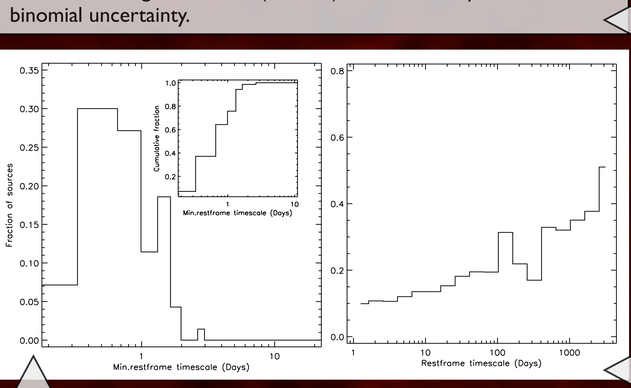

Fig.4: *Left:* Minimum detected variability timescales for sources with > 200 counts; we show the fraction of sources as a function of the shortest timescale on which the source is found to be variable. The inset shows the cumulative distribution. *Right:* Distribution of all variability timescales among CDFS sources with >200 cnts.

Simulating the Effect of Sparse Sampling and Low Statistics

The Excess Variance is commonly used in literature to estimate the intrinsic lightcurve variance:

$$\sigma^2_{NXV} = \frac{1}{N_{bin}\overline{x}^2} \sum_{i=1}^{N_{bin}} \left[(x_i - \overline{x})^2 - \sigma_i^2\right]$$

However this quantity represents the maximum likelyhood variability estimator only for identical/ normal distributed measurements errors and uniform sampling. In order to quantify the excess variance bias and uncertainty as variability estimator, in Allevato et al. (2013) we performed Monte Carlo simulations of realistic AGNs lightcurves. The simulations show (**Fig.6**) that variability measurements can be severely biased even in case of continuous monitoring), due primarily to red-noise leakage, and depending on the intrinsic power law slope. To recover the intrinsic variability amplitude such bias effect must be corrected for (see recipe in Allevato et al. 2013) using large samples or repeated measurements of the same source.

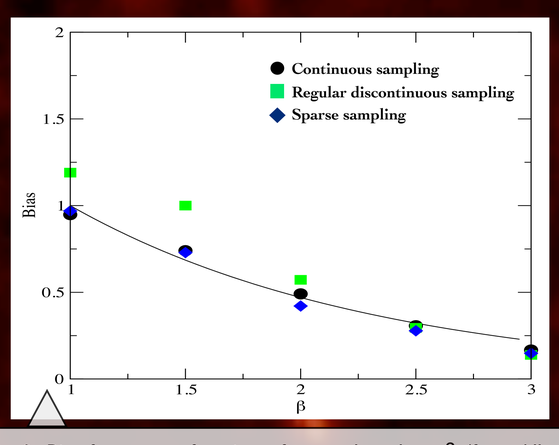

Fig.6: Bias factor as a function of power-law slope β (from Allevato et al. 2013). Different symbols represent the bias of the excess variance using different sampling patterns. The solid line shows the theoretical bias prediction. Note that actual measurements are biased also in the case of a continuously sampled lightcurve!

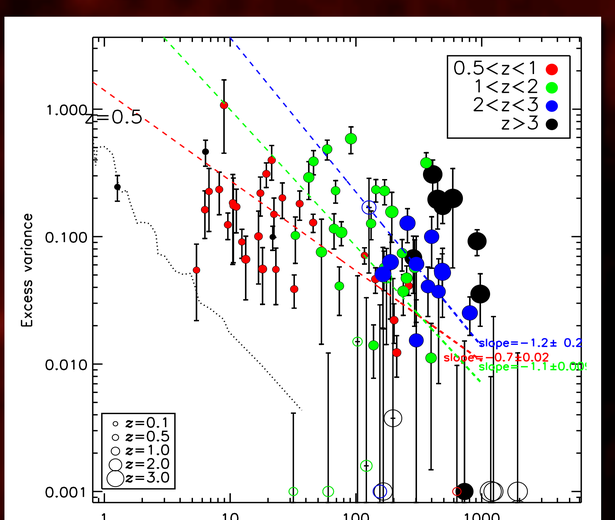

Fig.7: Luminosity-variability plot for the high-statistics CDFS sources. The line show the bisector fits in different redshift ranges

Variability dependence on redshift and AGN properties

The full 4Ms dataset allows to verify the variability-luminosity trends found at lower redshifts. In **Fig.7** we plot the measured excess variance against the intrinsic 0.5-7 keV luminosity for sources with > 600 net counts. The high threshold allows to derive robust measurements of the intrinsic variance, and selects a nearly complete sample of sources in terms of variability. We measured the variability-luminosity correlation through a weighted Least Squares Bisector for three subsamples with 0.5≤z<1.0, 1.0≤z<2.0 and 2.0≤z<3.0, finding respectively $\sigma^2_{NXV} \propto L^{-0.71\pm0.02}$; $\sigma^2_{NXV} \propto L^{-1.1\pm0.1}$ and $\sigma^2_{NXV} \propto L^{-1.2\pm0.2}$. In the low redshift range (0.5≤z<1.0) we find a close agreement with the values derived for local AGNs. The slopes of the higher redshift samples are steeper, but here the limited luminosity range does not allow to derive strong constrains.

In order to compare with more physically motivated models, we use those proposed by Papadakis et al. (2008) and Ponti et al. (2011), linking the luminosity and variability to the BH mass and accretion rates, but assuming different dependence of the PSD normalization. We compare the data (grouped in luminosity bins in order to include lower count-rate sources) to the models in **Fig.8** and **Fig.9**. Both models explain the anticorrelation with an increase in BH mass. However the Papadakis model requires an increase in accretion rate at high redshifts, while the Ponti model seems to fail to explain the redshift dependence. Alternatively the observed increase of variability with redshift could be the result of the bias shown in Fig. 6, due to the different timescales sampled at every redshift, if all AGNs possess a characteristic PSD break as observed in low redshift AGNs (Fig.1). Simulations to verify the importance of this effect are currently under way.

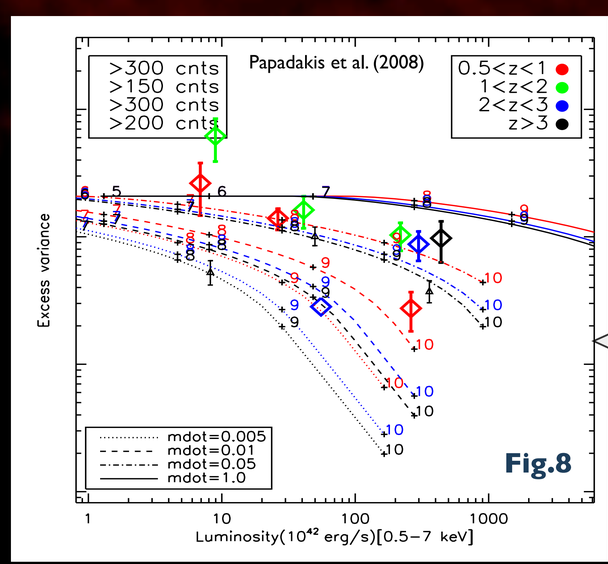

Fig.8

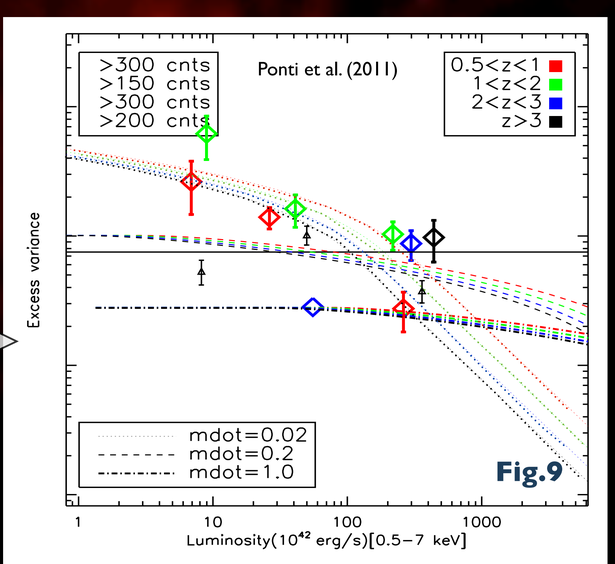

Fig.9